Improved Wear Resistance of the Fe-C-Ti Hardfacing Alloy by Nano TiCN Particles Fabricated by FCAW-N2

M. Mohammadikhah*

R & D Department, Kavosh Joosh Company, Tehran, Iran.
Received: 01 June 2018 - Accepted: 17 August 2018

Abstract

In this investigation the Fe-C-Ti hardfacing alloy was fabricated by FCAW-N_2 on AISI 1010 mild steel substrates, and then heat treatment was carried out on the samples. The OES, XRD, OM and SEM examinations and Rockwell hardness method were used for determining chemical composition, hardness and studying the microstructure of the hardface and heat treated samples. The OES examination results indicated that absorption of nitrogen in hardface sample was occurred. The XRD, OM and SEM examination results indicated that the microstructure of both hardface and heat treated sample, includes the ferrite with TiCN particles, but with different in size and distribute of the TiCN particles in microstructure. The microstructure of the heat treated sample had the nano scale of TiCN (500nm) with uniformly distribute at the ferrite matrix. The wear test (ASTM G 65) results indicate that the highest wear resistance is gained in the heat treated sample with maximum surface hardness. In addition, abrasive wear micromechanisms in steel substrate/ hardface / heat treated samples were recognized as: deep ploughing / ploughing + cutting / shallow ploughing + cutting respectively.

Keywords: Hardfacing, Nano TiCN, Abrasive Wear, Wear Micromechanism

1. Introduction

Wear is a process of progressive and undesirable loss or degradation of material from the surface of mechanical components, and therefore it is considered as one of the most significant surface failures of engineering parts [1,2]. Hardfacing is one of the methods used for controlling the wear failures of these parts [3]. Among the processes employed for hardfacing gas-shield flux core arc welding (FCAW) has become popular for many applications, because Numerous hardfacing materials are available and it, resulting in simplicity of operation [4]. The Fe-Cr-C, Fe-C-X (X: carbide former elements) and Fe-Ni-Co are three types of alloys that are used in the hardfacing of steel [5-7].

The Fe-C-X is one of the most popular alloys groups that used in the hardfacing of steel, because different alloys with various hardness and wear resistance can be fabricated [6]. The Fe-C-X alloys are used particularly in abrasive wear resistance conditions such as in the mining industries [6,7]. The abrasion wear resistance of The Fe-C-X alloys depends on the X element and characteristics of the hard phases in the microstructure [6-8]. Titanium has the great tendency form of the carbide and nitride, and when the carbon and nitrogen exist in chemical composition, the titanium prefers to be in the form of TiCN [9]. TiCN has cubic crystal structure (FCC B1 symmetry) with high bonding energy (13.7eV), therefore the TiCN has high hardness (2800HV) and melting point (2980°C), that can be used for the wear resistance applications[10,11].

Most investigations focus on the wear properties of the TiC or TiCN along with other elements at hardfacing alloys.Lee [12] suggested that Niobium and titanium have been used as the most effective carbonitride alloying elements, which can produce much hard precipitation if appropriate thermodynamic condition occur. Wang et al.[13] have produced the wear resistant clad layers on medium carbon steel by GTAW, where WC and TiC particles were directly added into the specified metal powders. The results showed that the TiC with W clad layer had superior wear performance under low sliding spee condition. Wang et al.[14] reported that in situ synthesized TiC particle reinforced composite coatings can be achieved under suitable welding parameters by GTAW on steel substrate. The TiC particles that formed from graphite and ferrotitanium uniformly distributed in the matrix and increased the hardness and abrasive wear resistance three to four times higher than that of 1045 steel substrate. Yang et al.[15] reported that carbonitride particles in the Fe-Cr-C(with Nb and Ti)hardfacing alloy ,are complex of Cr, Ti and Nb that distributed on the matrix with different size in as-welded and heat treated conditions. The size of the carbonitride particles in heat treated condition was finer than that as-welded condition and more decreased the wear rate. Although many researchers studied the production and wear properties of the TiC or TiCN along with other elements at microstructure of the hardfacing alloys, but the wear properties of TiCN (at nano scale) alone has not yet investigated.

*Corresponding author
Email address: m.mhd2965@yahoo.com

Therefore, this study presents the effect of nano TiCN particles on abrasion wear resistance of the Fe-C-Ti hardfacing alloy.

2. Materials and Methods

AISI 1010 low carbon steel (C=0.1%) specimens with the dimension of 400 ×200 × 10 mm were used as substrate.
Flux-cored wire with the combination materials that gives in Table. 1. used as filler metal. The FCAW with nitrogen gas used for fabricated of hardface layers on steel substrate. Table. 2. given hardfacing parameters by FCAW-N_2 process.

Table. 1. The combination materials (wt. %) of the cored wire.

Ferrotitanium	Graphite	Arc Stabilizers (Na_2CO_3+SiO_2)
80	10	10

Table. 2. The hardfacing parameters.

Process	FCAW
Cored Wire diameter(mm)	1.6
Number of passes	5(accordance ISO6847-2000)
Inter-pass temperatures (°C)	200
Polarity	DCEP
Welding Voltage(V)	29
Welding Current(A)	310
Wire Extension(mm)	19
Welding Speed(mm/min)	330

After hardfacing, samples cut from top of the hardface specimens and heat treated at 1000°C for 1 hour in an electric furnace (Fig. 1.).

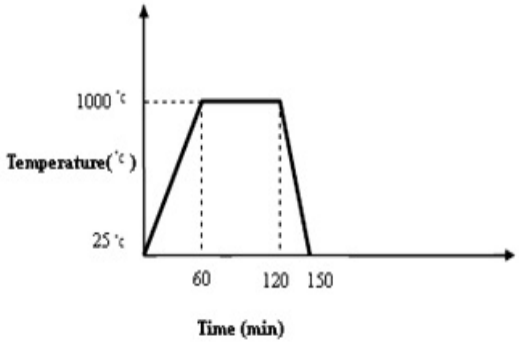

Fig. 1. Schematic of Heat treatment cycle.

Chemical analysis of Samples was carried out by an optical emission spectrum (OES) equipped with the charge-coupled device (CCD) technology.

In addition, the nitrogen absorption content in the weld metal was measured by using of nitrogen/oxygen determinate equipment. The X-ray diffraction (XRD) samples were prepared by mechanical and electro polishing [16].
The XRD examination was carried out by a diffractometer (Philips 332) using copper K-alpha k=1.54A° radiation and a nickel filter. The XRD examination was performed using an angle of 10–80° with the step size of 0.02° and a time step of 10s per each step. The metallographic samples were prepared by using SiC grinder paper, 1µm diamond paste polisher, 2% nital solution etchant.
The microstructure characterization of each sample was studied by an optical microscope (Olympus-CK 40M) equipped with image analysis software and a scanning electron microscope (VEGA-TESCAN) using backscattered electrons (BSE), energy-dispersive spectroscopy (EDS) analysis with 20 kV accelerated voltage.
The macro hardness test (HVS 1000) was performed by using Rockwell hardness tester with 100 kg force. The abrasive wear test was performed in a dry sand–rubber wheel testing machine (Fig. 2.) in accordance with the ASTM G65 standard. The parameters of the abrasive wear test are given in Table. 3.

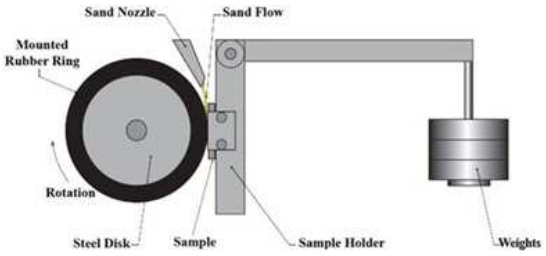

Fig. 2. Schematic of the dry sand–rubber testing machine, in accordance with the ASTM G65 standard.

Table. 3. Abrasive wear test conditions.

Parameter	Value
Condition:	
Velocity	200 rpm
Load	130 N
Sand flow	300 gr/min
Wear distance	4309 m
Wheel diameter	225 mm
Abrasive particles:	
Type	Quartz
Size	210-300 µm
Hardness	1000-1100 HV
Shape	Rounded
Sample dimensions:	75×25×10 mm

The abrasive wear resistance was determined from the mass loss results that were measured with 0.01 mg resolution. In addition, after the wear test, the worn surface was observed by SEM in order to

determine micromechanism of wear for each sample.

3. Results and Discussion

Table. 4. provides chemical analysis (wt. %) of steel substrate and hardface layer.

Table. 4. Chemical analysis (wt. %) of steel substrate and hardface layer.

sample	C	Mn	Si	Ti	N	Fe
AISI 1010	0.11	0.55	0.32	-	-	Bal
Hardface layer	0.67	0.31	0.15	6.58	0.14	Bal

It is noted that hardface sample has nitrogen in chemical analysis, and absorption nitrogen in hardface sample was occurred, this is due to the presence of the ferrotitanium that was used as combination materials (Table. 1.) in cored wire.
Fig. 3. shows the XRD pattern of the hardface sample. It can be seen that peaks of TiCN with ferrite (C -Fe) are present in the hardface layer. The ferrite phase formation related as: [9,17,18].

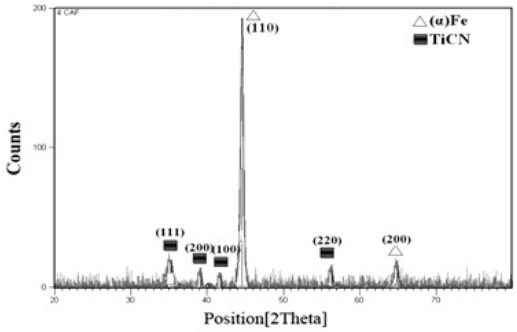

Fig. 3. XRD pattern of hardface sample.

a. carbon concentration reduce at solid phase (austenite) by formation of TiCN in melt.
b. low cooling rate created by using interpass temperature in hardfacing process(Table. 2.).
Fig. 4. shows the Gibbs free energy formation of different nitrides and carbides.
It can be seen that titanium has the lowest free energy to formation of nitride and carbide, from other elements. Therefore at presence of nitrogen, and carbon together, titanium content in melt do not allow to combination of other elements and TiCN formation at the melt. Fig. 5. shows the microstructure of hardface sample.
It can be seen that microstructure of hardface sample consist of ferrite, and some cubical TiCN particles with size 1 to 3µm. Fig. 6. shows the EDS point analysis of the matrix (ferrite) and particles (TiCN) of the microstructure in hardface sample.

The EDS analysis illustrates that the matrix (ferrite) was enriched with the Fe element and particles (TiCN) were enriched of Ti element.

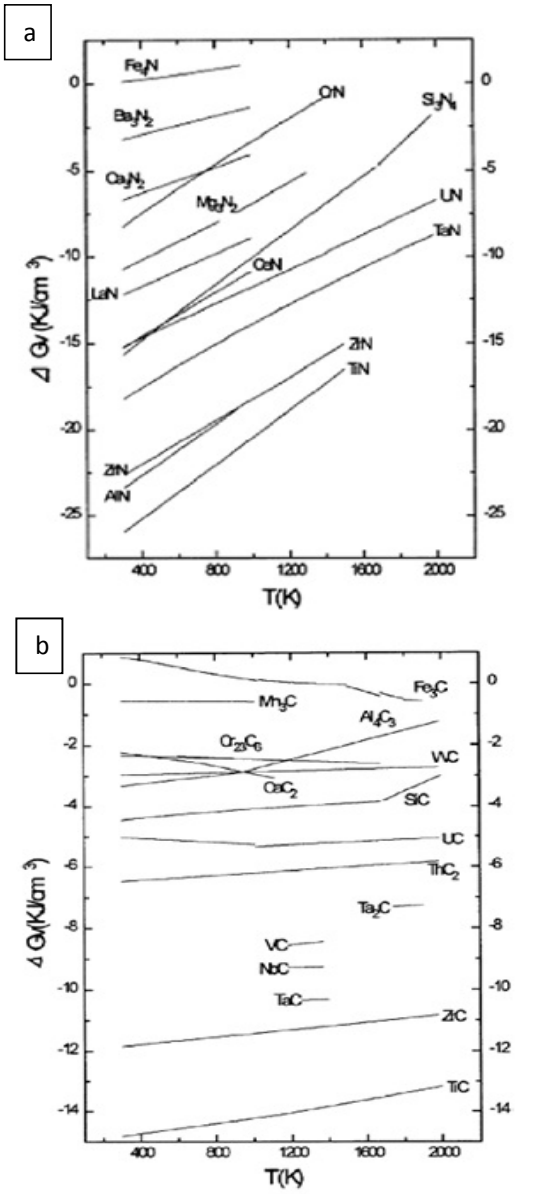

Fig. 4. Gibbs free energy formation of different (a) nitrides and (b) carbides [18].

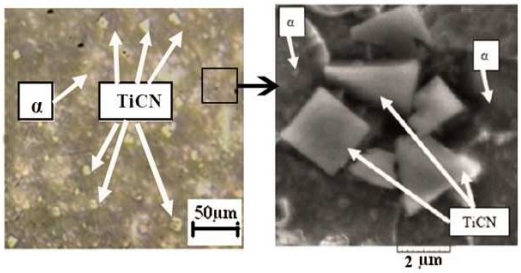

Fig. 5. The OM and SEM micrograph of hardface sample.

Fig. 7. shows the mapping elements of the microstructure of the hardface sample, it can be seen that Fe element is concentrated in matrix and Ti is concentrated in TiCN particles, C and N elements are dispersed at both of the matrix and TiCN particles uniformly.

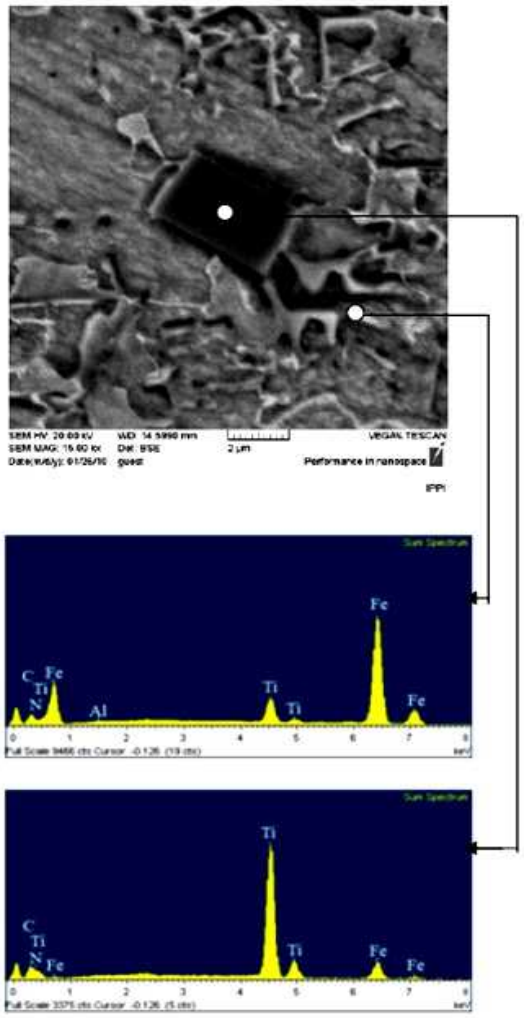

Fig. 6. the EDS point analysis of the matrix (ferrite) and particles (TiCN) of the hardface sample microstructure.

Fig. 8. shows the microstructure of heat terated sample. It can be seen that the microstructure of the heat treated sample includes the fine TiCN particles with cubical and hemispherical shapes at nano scale (~500nm) that distributed more uniformly in the ferrite matrix. In fact the heat treatment can reduce the size of TiCN particles and uniformly distributed them at microstructure. According to Fe-Ti-C-N phase diagram [19], at 970°C the eutectic transformation occur and C , N atoms tendency to leave the crystal structure and diffusion to the matrix[9,15], therefore the size of TiCN particles are reduce and shape of them be changed to hemispherical. The hardness of different samples is shown in Fig. 9. It can be seen that the hardness of hardface sample is 49 HRC and heat treated sample is 58 HRC and hardness of both sample are greater than that hardness of steel substrate (18 HRC).

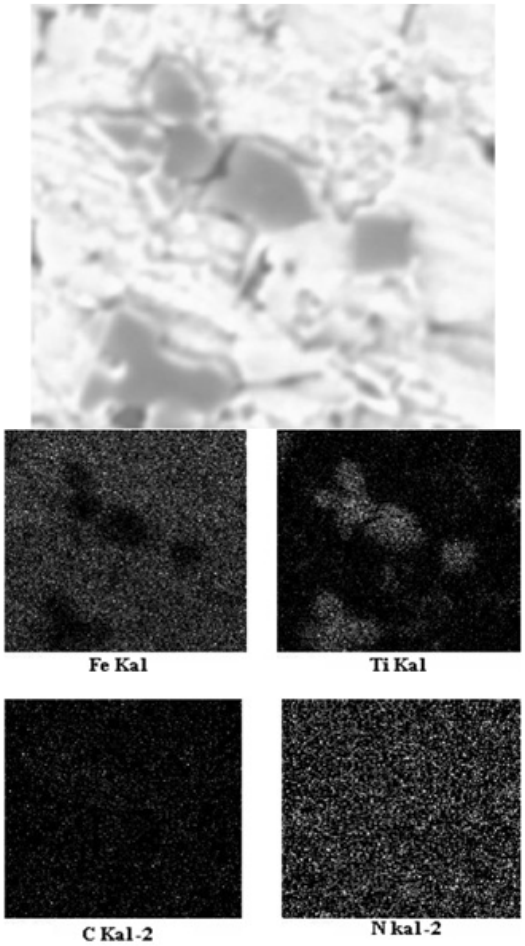

Fig. 7. The mapping elements of the hardface sample microstructure.

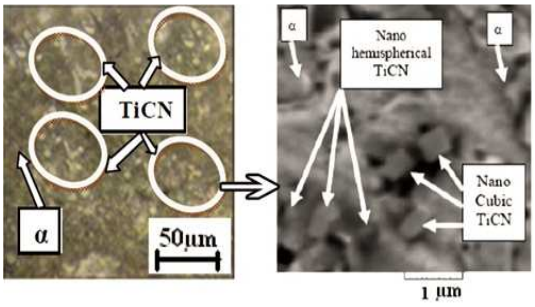

Fig. 8. The OM and SEM micrograph of heat treated sample.

The TiCN contribute to the higher hardness values of hardfacing alloys [9,11] and hence, the improvement of hardness in hardface and heat treated sample is affected by TiCN in the microstructure.

In addition, Fig. 9. shows that the hardness of heat treated sample is higher than that hardface sample. This due from size and distribute of TiCN particles in microstructure. By comparing of the Fig. 5. and Fig. 8. is determined that the size of TiCN particles in heat treated sample microstructure is finer (~500 nm) and more uniformly distribute at the ferrite matrix than that the hardface sample microstructure.

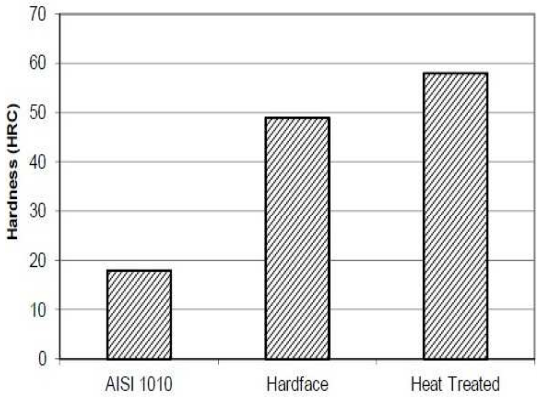

Fig. 9. Hardness of the different samples.

Fig. 10. shows the weight loss of hardface, heat treated and steel substrate (AISI 1010) samples after 4309 m wear distance. This value shows that AISI 1010 has a low abrasive wear resistance, these indicate that TiCN hard phases in the ferrite matrix can be controlled the wear rate. In addition, it can be seen that the highest wear resistance was achieved in heat treated sample.

This due to nano size TiCN particles with uniformly distribution at microstructure**,** because when the particles are the nano sizes, the surface contact of the particles during wear test increases[15], and since the TiCN is hard phase(2800 HV) [11], the abrasive wear resistant increases.

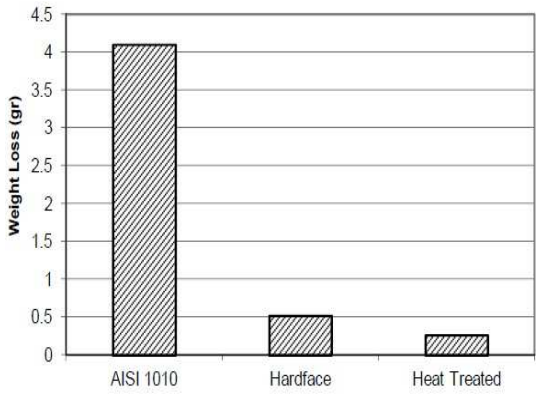

Fig. 10. Weight loss of different samples in 4309m wear distance.

The worn surface morphology is related to the wear micromechanism. Fig. 11. shows the worn surface of AISI 1010 mild steel. Continuous deep scratches can be observed on the worn surface, therefore the deep ploughing is the main abrasive wear micromechanism.

Fig. 12. shows the worn surface of hardface sample. Discontinuous scratches with craters can be seen on the worn surface, hence, the ploughing and cutting are the main abrasive wear micromechanism for this sample.

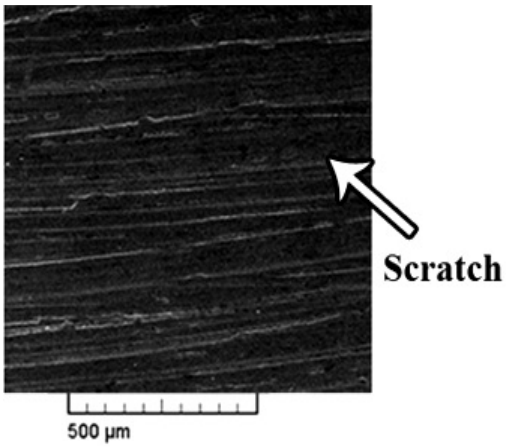

Fig. 11. SEM micrographs of the worn surface of AISI 1010 mild steel.

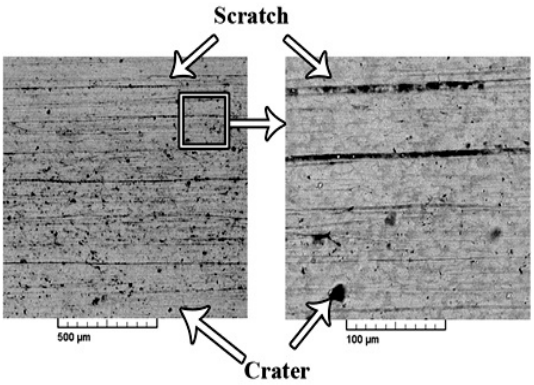

Fig. 12. SEM micrograph of the worn surface of hardface Sample.

It can be seen that the TiCN cuts from the matrix. This is because microstructure is composed of ferrite and TiCN particles with different thermal expansion coefficient and plastic strain rate[9]. Therefore, stress formation at the Ferrite/TiCN interface occurs during the wear test which is due to cutting and separation of the brittle phase as TiCN from the microstructure at the surface.

Fig. 13. shows the worn surface of heat treated sample. Discontinuous shallow scratches with craters may be observed on the worn surface.

Therefore the shallow ploughing with cutting is the main abrasive wear micromechanism of this sample.

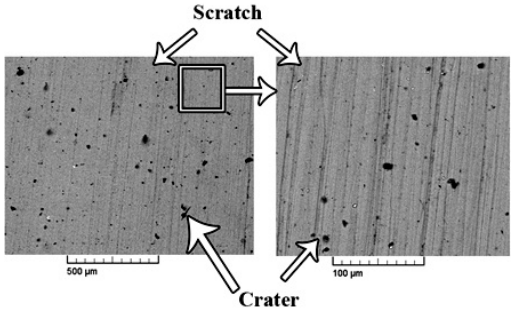

Fig. 13. SEM micrograph of the worn surface of heat treated Sample.

It can be seen that the TiCN particles cuts from the matrix. Similarly of hardface sample, TiCN particles separates from the microstructure due to stress formation at the Ferrite/TiCN interface during wear test.

4. Conclusions

From the results of a study abrasive wear resistance of the Fe-C-Ti hardfacing alloy contains of TiCN particles at microstructure, the following conclusions can be drawn:

1. TiCN particles can be formed by using of nitrogen gas with cored wire contains of the ferrotitanium in FCAW-N_2 process.
2. The microstructure of both hardface and heat treated sample, includes the ferrite with TiCN particles, but with different in size and distribution of the TiCN particles in microstructure.
3. By heat treatment, the size of TiCN reduce to very fine scale (~500nm) with more uniformly distribution at the ferrite matrix in the microstructure hence the surface hardness is increased.
4. The wear test results indicate that the minimum weight loss and the highest abrasive wear resistance are achieved by heat treated sample with contains of the nano size TiCN particles in microstructure.
5. The SEM observation of the worn surface indicates that steel substrate/ hardface / heat treated samples have the abrasive wear micromechanisms as: deep ploughing / ploughing+cutting / shallow ploughing+cutting, respectively.

References

[1] J. B. Cheng, B. S. Xu, X. B. Liang and W. Wu, Mat. Sci. Eng., A492 (2008), 407.
[2] Y. F. Liu, Z. Y. Xia, J. M. Han, G. L. Zhang and S. Z. Yang, Surf. Coat. Tech., 201, (2006), 863.
[3] J. J. Coronado, H. F. Caicedo and A. L. Gomez, Trib. Int., 42 (2009), 745.
[4] A. Klimpel, L. A. Dobrzanski, J. Mat. Proc. Tech., 164 (2005), 1056.
[5] H. Sabet, S. Khierandish, S. Mirdamadi, M. Goodarzi, Trib. Lett., 44 (2011), 237.
[6] A. S. C. M. D'Oliveira, J. J. Tigrinho and R. R. Takeyama, Surf. Coat. Tech., 202 (2008), 4660.
[7] W. Zmudzinski, M. Ezekiel, Mat. Forum., 30(2006), 333.
[8] J. Chen, P. Hua, P. Chen, C. Chang, M. Chen and W. Wu, Mat. Lett., 62 (2008), 2490.
[9] M. Mohammadikhah, H. Sabet, A. Shokouhfar A. Hadizadeh and S. Mehrabeian, AWST-10/107, Int. Con. IIW, 11-17 (2010), 523.
[10] S. T. Oyama, J. Sol. Stat. Chem., 96 (1992), 442.
[11] H. O. Pierson, Handbook of Refractory Carbides and Nitrides, Properties and Characteristics, pp100-115 Noyes Publications, Newjersy (1996)
[12] B. J. Lee, Met. Mat. Trans., 32A(2001), 2423.
[13] S. W. Wang, Y. C. Lin and Y. Y. Tsai, J. Mat. Proc. Tech., 140 (2003), 682.
[14] X. H. Wang, S. L. Song, Z. D. Zou and S. Y. Qu, Mat. Sci. Eng., A 441 (2006), 60.
[15] K. Yang, S. Yu, Y. Li, C. L. Li, App. Sur. Sci., 254 (2008), 5023.
[16] H. Sabet, S. Mirdamadi, S. Khierandish and M. Goodarzi, J. App. Chem. Res., 15 (2010), 70.
[17] K. S. Bang, C. Park and S. Liu, J. Mat. Sci., 41(2006), 5994.
[18] Y. He, Z. Li, H. Qi, W. Gao, Mat. Res. Innovat., 1(1997), 157.
[19] V. Raghavan, J. Pha. Equ., 24 (2003), 75.